CHIN. PHYS. LETT. Vol. 38, No. 1 (2021) 014401 **Express Letter**

How Does van der Waals Confinement Enhance Phonon Transport?

Xiaoxiang Yu(余晓翔)[1,2†], Dengke Ma(马登科)[1,3†], Chengcheng Deng(邓程程)[2*], Xiao Wan(万骁)[2], Meng An(安盟)[1,4], Han Meng(孟涵)[2], Xiaobo Li(李小波)[2], Xiaoming Huang(黄晓明)[2*], and Nuo Yang(杨诺)[1,2*]

[1]*State Key Laboratory of Coal Combustion, Huazhong University of Science and Technology, Wuhan 430074, China*
[2]*School of Energy and Power Engineering, Huazhong University of Science and Technology, Wuhan 430074, China*
[3]*NNU-SULI Thermal Energy Research Center (NSTER) & Center for Quantum Transport and Thermal Energy Science (CQTES), School of Physics and Technology, Nanjing Normal University, Nanjing 210023, China*
[4]*College of Mechanical and Electrical Engineering, Shaanxi University of Science and Technology, Xi'an 710021, China*

(Received 6 October 2020; accepted 12 November 2020; published online 25 November 2020)

We study the mechanism of van der Waals (vdW) interactions on phonon transport in atomic scale, which would boost developments in heat management and energy conversion. Commonly, the vdW interactions are regarded as a hindrance in phonon transport. Here we propose that the vdW confinement can enhance phonon transport. Through molecular dynamics simulations, it is realized that the vdW confinement is able to make more than two-fold enhancement on thermal conductivity of both polyethylene single chain and graphene nanoribbon. The quantitative analyses of morphology, local vdW potential energy and dynamical properties are carried out to reveal the underlying physical mechanism. It is found that the confined vdW potential barriers reduce the atomic thermal displacement magnitudes, leading to less phonon scattering and facilitating thermal transport. Our study offers a new strategy to modulate the phonon transport.

DOI: 10.1088/0256-307X/38/1/014401

It is well known that van der Waals (vdW) interactions, which arise from the electromagnetic forces between quantum fluctuation-induced charges,[1] exist in reality universally, and they play a significant role in many diverse fields such as condensed matter physics,[2–6] reaction's dynamics in chemistry[7] and assembly of complex supramolecule in biology.[8] In the area of heat transfer, vdW interactions can remarkably impact phonon transport in nanostructured materials due to their large surface-to-volume ratios.[9,10] Phonon transport in nanoscale is of great importance to many practical applications, including energy conversion and package of electronics.[11–15] Generally, nanomaterials are utilized in specific forms like in-bundles or with-substrates, where there are inevitable vdW interactions. Hence, there are intense demands to understand how vdW interactions affect phonon transport in nanostructured materials.

Tremendous efforts have been devoted to research of this topic in past decades.[16] Commonly, theoretical and experimental studies concluded that vdW interactions block phonon transport and lead to a reduction of thermal conductivity (TC) in nanostructures.[17–23] Recently, Yang *et al.* and Zhang *et al.* experimentally demonstrated an enhancement of TC by vdW interactions for graphene-like h-BN nanoribbon[24] and quasi-1D vdW crystal $Ta_2Pd_3Se_8$ nanowires,[25] respectively. For understanding their effect on phonon transport, there have been only a few studies on the intensity of vdW interactions by simulating Frenkel–Kontorova lattices[26] and Fermi–Pasta–Ulam chains.[27]

In this Letter, we theoretically study how vdW interactions modulate, especially enhance, the phonon transport in nanoscale. Firstly, a strategy on artificially designing the nanostructures is proposed. Secondly, based on equilibrium molecular dynamics (EMD) simulations on typical nanostructures designed by the strategy, we show that the vdW interactions may enhance phonon transport. Lastly, to reveal the underlying physical mechanism, we present the quantitative analyses of morphology, local vdW potential energy and dynamical properties.

We propose a new vdW confinement effect that the vdW interactions could form potential barriers on atoms, thus may confine the vibrational amplitude, which will decrease anharmonic phonon scattering and facilitate thermal transport. The vdW potential barriers can be made by artificially designing the nanostructures. Therefore, a proper designing strategy is the key issue. In the following, an alternative artificial structure, named as the crosswise paved laminate (CPL), is introduced. The TCs of CPL structures are obtained by EMD simulations, which are compared

Supported by the National Natural Science Foundation of China (Grant Nos. 51606072 and 51576077).
†Xiaoxiang Yu and Dengke Ma contributed equally to this work.
*Corresponding authors. Email: dengcc@hust.edu.cn; xmhuang@hust.edu.cn; nuo@hust.edu.cn

with TCs of other corresponding structures, such as single-chain polyethylene (SC-PE)[28] and single-layer graphene nanoribbon (SL-GNR).

The CPL structures are constructed based on PE chains and GNRs, respectively [see details in section 1 of the Supplementary Information (SI)]. As depicted in Figs. 1(a) and 1(b), the aligned chains or ribbons are paved layer by layer, and the aligned directions are crosswise for two adjacent layers. The intersection angle of PE chains is 90°, while that of GNR is set to 120° due to ordered stacking of its hexagonal structure. It is worth noting that the CPL structures are probably fabricated (see details in section 2 of the SI) according to a recent experimental research on the weaving of organic threads.[29] Also, there have already been analogous structures reported, such as orthogonal self-assembly multilayer polymer meshes[30] and ordered polymer structure.[31]

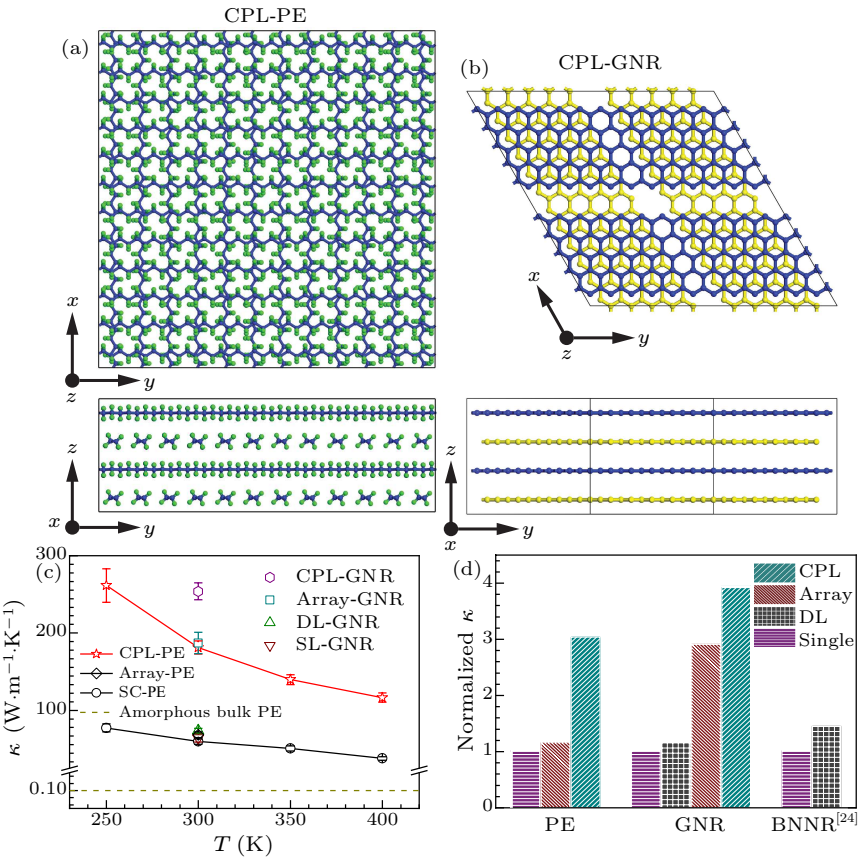

Fig. 1. (a) and (b) Schematic views of simulation cell of crosswise paved laminate (CPL) for polyethylene (PE) chain and graphene nanoribbon (GNR), respectively. (c) The thermal conductivities of PE chains and GNR systems versus temperature. (d) The ratios of thermal conductivity for structures with [CPL, array and double layer (DL)] and without vdW interactions (single chain/ribbon).

The TCs of CPL structures were calculated by the Green–Kubo formula[32] using the LAMMPS package[33] (simulation details are given in section 3 of the SI). Although the validation of the Green–Kubo formula for low-dimensional systems remains inconclusive,[34–36] there have been many studies on thermal transport in both nanostructures and bulk materials.[37,38] We do not discuss this issue here. The inter-atomic interactions in PE and GNR are described by the adaptive intermolecular reactive bond order (AIREBO) potential,[39–42] which provides a realistic description of the dynamics and anharmonicity.[43,44] To accurately simulate an infinite system with a finite MD simulation cell, periodic boundary conditions are applied along all three directions, which inhibit phonons from being attenuated by boundaries. Length dependence of TC is investigated to overcome the size effect (see details in section 4 of the SI). The TCs of CPL structures along two in-plane directions (x and y) are much higher than that along cross-plane direction (z) ($<1\,\mathrm{W\cdot m^{-1}\cdot K^{-1}}$) contributed by nonbonding interactions. Thus we only focus on the TCs of CPL structures along two in-plane directions throughout this study.

As shown in Fig. 1(c), the TC of SC-PE and SL-GNR are $54\,\mathrm{W\cdot m^{-1}\cdot K^{-1}}$ and $64\,\mathrm{W\cdot m^{-1}\cdot K^{-1}}$ at room temperature, respectively. The $\kappa_{\mathrm{SC-PE}}$ is comparable to the previous simulation studies.[45,46] The

value of $\kappa_{\mathrm{SL-GNR}}$ is slightly smaller than the previous simulation result using the same methods,[20,44,47] which is ascribed to a smaller width and size confinement effect. With the effect of vdW interactions, the TCs of both PE and GNR systems gradually increase for arrays and CPL structures. Especially, the TCs of CPL structures for PE and GNR are several times larger than that of single ones, due to vdW confinement which decreases phonon scattering as will be discussed later in detail. At room temperature, $\kappa_{\mathrm{CPL-PE}}$ and $\kappa_{\mathrm{CPL-GNR}}$ reach as high as 181 $\mathrm{W{\cdot}m^{-1}{\cdot}K^{-1}}$ and 254 $\mathrm{W{\cdot}m^{-1}{\cdot}K^{-1}}$ respectively. Both SC-PE and CPL-PE show negative temperature dependence of TC. Moreover, the values of $\kappa_{\mathrm{CPL-PE}}$, e.g., 181 $\mathrm{W{\cdot}m^{-1}{\cdot}K^{-1}}$ at 300 K, are conservatively calculated using the whole bulk cross section area. When we consider the contribution of each layer to the thermal transport, the layers, where PE chains are perpendicular to direction of heat transfer, have an ultralow TC. Thus, most of the contributions come from the layers where PE chains are parallel to the direction of heat transfer, whose TCs are estimated to be twice of $\kappa_{\mathrm{CPL-PE}}$, such as $\sim$362 $\mathrm{W{\cdot}m^{-1}{\cdot}K^{-1}}$ at 300 K. The possible high TC of the CPL structure for GNR can be predicted in the similar way. Furthermore, the CPL structures have high TCs along two in-plane directions, adding an extra dimension for efficient heat dissipation. To some extent, high TC along two directions means one effective way of enhancement of thermal properties.

Moreover, due to vdW potential barriers, Fig. 1(d) presents the enhancement ratios of TC for PE chains, GNRs and boron nitride nanoribbons (BNNRs), respectively. Compared with the SC/SL structure, array-PE has slightly improvement of TC, while array-GNR shows almost two times increase in TC. Especially, CPL-PE and CPL-GNR respectively exhibit two times and nearly three times enhancement on TC. In addition, the TC of DL-GNR is higher than that of SL-GNR, which is consistent with the experimental result of SL and DL graphene-like hexagonal boron nitride nanoribbon.[24]

To gain insights into the phonon transport enhancement, the mechanism of vdW confinement will be shown in the following. Herein, we only show the results about PE in the main body to avoid repeated description of similar results about GNR (shown in the SI). The morphology of PE chains is quantified to exhibit atomic vibrations through radial distribution functions (RDFs) (calculation details are given in section 5 of the SI) and probability distribution of the dihedral angle of the C–C–C–C backbone. Figure 2(a) shows the significant differences of lattice orders between SC-PE and CPL-PE. For SC-PE, there is no obvious peak in RDFs. Correspondingly, the distribution along the chain axis (blue dots) indicates that atomic vibrations in SC-PE are full of bending motions. In contrast, there are two sharp peaks in RDFs of one PE chain in CPL-PE. According to the distribution along the chain axis (red dots), the two peaks in RDFs of CPL-PE correspond to the equilibrium positions at which C atoms and H atoms are located (green circles). This denotes that CPL-PE has more crystal-like atomic vibrations of hydrogen atoms and subdued bending motion of backbone than SC-PE, which is conducive to a higher TC. Moreover, from the probability distributions of the dihedral angles of the backbone as shown in Fig. 2(b), there is a much steeper peak for one chain in CPL-PE than the SC-PE. This means that there is much weaker torsional motion of one PE chain in CPL-PE than in SC-PE. In brief, vdW confinement enables CPL-PE more crystal-like. The long-range order is a crucial factor for phonon transferring in low-dimensional dielectrics and semiconductors, such as SC-PE and SL-GNR. The thermal fluctuation would break the long-range order and induce strong phonon scattering. Through designing confined vdW potential barriers in artificial CPL structures, it is demonstrated that the long-range order could be increased by the vdW confinement effect, which weakens phonon scattering and enhances thermal conductivity.

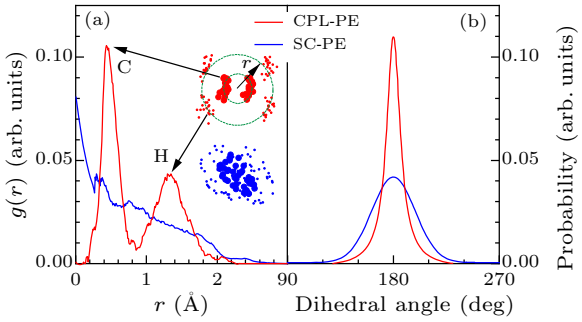

Fig. 2. (a) Radial distribution functions (RDFs) $g(r)$ of carbon and hydrogen atoms and (b) probability distributions of dihedral angles of C–C–C–C backbone in PE chain.

To elaborate the vdW confinement in CPL, we analyze the potential energy barrier of both CPL-PE and array-PE (calculation details are given in section 6 of the SI). The local potential energy barrier is mapped to evaluate the confinement on atomic vibrations by vdW interactions. For translational motion, there is an obvious confined vdW potential barrier in CPL-PE [Fig. 3(a)], while the array-PE shows small potential change along y direction [Fig. 3(b)]. Compared to CPL-PE, atoms in array-PE can move easily along y direction, thus there is less vdW confinement. This discrepancy stems from the unidirectional alignment of array-PE and crosswise layout of CPL-PE, which indicates that CPL-PE could confine the atomic motions more effectively than array-PE. CPL-GNR also shows

confined potential energy barriers (given in section 7 of the SI). To evaluate the effect of thermal fluctuation, the vdW potential barriers in two structures at 300 K are also calculated, as shown in Fig. S4. According to Figs. S4(a) and S4(c), the vdW potential barriers of CPL are stable with thermal fluctuations, which verifies that the vdW confinement effect works well at room temperature. Furthermore, Fig. 3(c) demonstrates the comparison of potential energy changes of PE chain in CPL-PE and array-PE as a function of rotation angle. As can be seen, CPL-PE shows bilateral steeper potential barrier than array-PE. Thus, the CPL structure can confine the segmental rotation better, thus diminish anharmonic phonon scattering, which facilitates thermal transport.

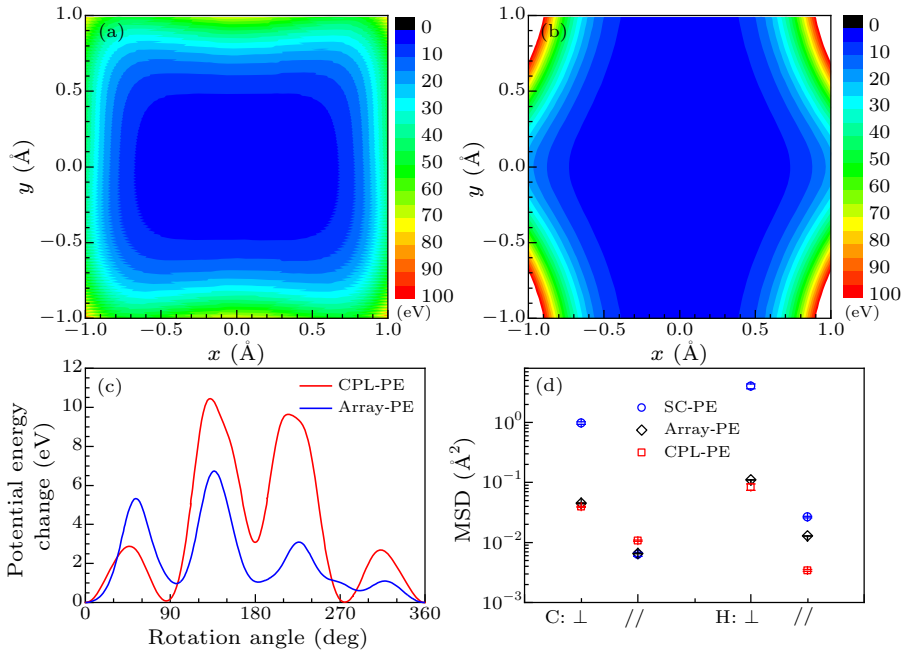

Fig. 3. The potential energy barriers of PE chain in (a) CPL-PE and (b) PE array. (c) The potential energy changes as a function of rotation angle. There is a confined vdW potential barrier in CPL-PE in comparison with PE array. (d) The mean square displacement (MSD) along radial (⊥) and axial (∥) directions of carbon and hydrogen atoms.

To shed further light on the anharmonic properties, we calculate mean square displacement (MSD) through MD simulations including full anharmonicity by directly using time-averaging positions. Since the atoms are only allowed to displace from equilibrium through the natural energy of the thermal fluctuations, the closer the atom deviates from the equilibrium position, the less the phonon-phonon scattering occurs, which means the system is less anharmonic.[48,49] As shown in Fig. 3(d), the MSD of PE chains in CPL-PE, especially that of hydrogen atoms, is much smaller than that of SC-PE. Recent theoretical work emphasized that large thermal displacements of hydrogen strongly affect motion of carbon atoms, thereby altering the scattering phase space and reducing the TC.[49] In our work, the thermal displacements of hydrogen atoms are reduced by vdW confinement and thus cause the TC enhanced.

Last but not least, we would like to provide a predictive framework, namely, two implications of applying our designing strategy to achieve vdW confinement. On the one hand, the preferable materials to achieve positive effect of vdW confinement on thermal transport would better have two characteristics: (i) extremely large surface-to-volume ratio, like one-dimensional (1D) and quasi-1D nanostructures; (ii) stiff along axial direction while soft along radial direction, namely, potentially good thermal transport along axial direction but strong phonon scattering by anharmonic radial atomic vibration. The first characteristic leads to considerable effect of vdW interactions. The second characteristic ensures the possibility to improve TC via vdW interactions. On the other hand, the preferable structures that are conducive to forming strong confined vdW potential barrier, are radially parallel, axially crosswise and periodically ordered layout, e.g., CPL. The parallel structures enable the vdW barriers ordered, thus confine the anharmonic atomic vibration by each other. Meanwhile, the crosswise structure is able to diminish the torsional motion better. Furthermore, periodically ordered structure could further strengthen vdW confinement effect. Bottom-up manufacture is an alternative feasible method to fabricate such structures.[29,30]

In conclusion, we have proposed a new mechanism, van der Waals confinement, to enhance phonon transport. The vdW confinement originates from the potential barriers formed by ordered vdW interactions, which leads to a confinement of atomic thermal vibrational displacement. Thus, the vdW confinement could modulate phonon transport and the propagation of energy carriers. An alternative artificial CPL structure is established based on the vdW confinement. The EMD simulation results show that the thermal conductivities of CPL structures for PE and GNR systems at room temperature ($181\,\mathrm{W\cdot m^{-1}\cdot K^{-1}}$ and $254\,\mathrm{W\cdot m^{-1}\cdot K^{-1}}$) are two-fold and three-fold as those of SC-PE and SL-GNR, respectively. Morphology analyses exhibit that the atomic thermal vibration is confined, which means the reduction of anharmonicity in the system. Through mapping the potential energy, it is found that the CPL structures present confined vdW potential barriers, namely strong vdW confinement, making the atomic thermal vibrations more crystal-like. Furthermore, the CPL structures have excellent thermal properties along two directions, which goes a step further in the enhancement of thermal transport and extends the scope of applications. Polymers with high thermal conductivity may also have other technological advantages such as low cost, light weight, electrical insulation and chemical stability, so our work provides promising alternative materials to solve the crucial heat dissipation issue which is the major reason for the breakdown of micro/nanoelectronic devices. We have studied how vdW interactions can modulate the transport of heat carriers/phonons, which will be of great general interest to both experimentalists and theorists in a broad field, such as phononics,[50] thermoelectrics,[51,52] and multi-carrier nonequilibrium dynamics.[53,54] Moreover, the vdW confinement giving rise to the recovery of crystal-like atomic vibrations may weaken the electron-phonon scattering thus boost the electrical transport,[55,56] which is important for polymer-like soft materials in flexible electronics. Additionally, photoelectric properties of soft materials in organic solar cells and light emitting diodes may also be influenced by morphologies[57,58] and thus could be modulated by vdW confinement.

The authors thank Quanwen Liao for stimulating discussion, and are grateful to the National Supercomputing Center in Tianjin (NSCC-TJ) and China Scientific Computing Grid (ScGrid) for providing help in computations.

References

[1] Zhao R, Luo Y, Fernandezdominguez A I and Pendry J B 2013 *Phys. Rev. Lett.* **111** 033602
[2] Beguin L, Vernier A, Chicireanu R, Lahaye T and Browaeys A 2013 *Phys. Rev. Lett.* **110** 263201
[3] Rao A M, Chen J, Richter E, Schlecht U, Eklund P C, Haddon R C, Venkateswaran U D, Kwon Y K and Tomanek D 2001 *Phys. Rev. Lett.* **86** 3895
[4] Woods L M, Dalvit D A R, Tkatchenko A, Rodriguez-Lopez P, Rodriguez A W and Podgornik R 2016 *Rev. Mod. Phys.* **88** 045003
[5] Cardoso C, Soriano D, García-Martínez N A and Fernández-Rossier J 2018 *Phys. Rev. Lett.* **121** 067701
[6] Mi X Y, Yu X, Yao K L, Huang X, Yang N and Lü J T 2015 *Nano Lett.* **15** 5229
[7] Lee J H, Avsar A, Jung J, Tan J Y, Watanabe K *et al.* 2015 *Nano Lett.* **15** 319
[8] Stornaiuolo M, De Kloe G E, Rucktooa P, Fish A, van Elk R *et al.* 2013 *Nat. Commun.* **4** 1875
[9] Seol J H, Jo I, Moore A L, Lindsay L, Aitken Z H *et al.* 2010 *Science* **328** 213
[10] Zhang X, Bao H and Hu M 2015 *Nanoscale* **7** 6014
[11] Ambrosetti A, Ferri N, Distasio R A and Tkatchenko A 2016 *Science* **351** 1171
[12] Baxter J, Bian Z X, Chen G, Danielson D, Dresselhaus M S *et al.* 2009 *Energy & Environ. Sci.* **2** 559
[13] Yang L, Yang N and Li B 2014 *Nano Lett.* **14** 1734
[14] Ma D, Ding H, Meng H, Feng L, Wu Y, Shiomi J and Yang N 2016 *Phys. Rev. B* **94** 165434
[15] Dresselhaus M S, Chen G, Tang M Y, Yang R, Lee H, Wang D, Ren Z, Fleurial J P and Gogna P 2007 *Adv. Mater.* **19** 1043
[16] Shao C, Yu X, Yang N, Yue Y and Bao H 2017 *Nanoscale Microscale Thermophys. Eng.* **21** 201
[17] Lindsay L, Broido D A and Mingo N 2011 *Phys. Rev. B* **83** 235428
[18] Ghosh S, Bao W, Nika D L, Subrina S, Pokatilov E P, Lau C N and Balandin A A 2010 *Nat. Mater.* **9** 555
[19] Kuang Y, Lindsay L and Huang B 2015 *Nano Lett.* **15** 6121
[20] Yang N, Ni X, Jiang J W and Li B 2012 *Appl. Phys. Lett.* **100** 093107
[21] Hsu I K, Pettes M T, Bushmaker A, Aykol M, Shi L and Cronin S B 2009 *Nano Lett.* **9** 590
[22] Lindsay L and Broido D A 2012 *Phys. Rev. B* **85** 035436
[23] Fujii M, Zhang X, Xie H, Ago H, Takahashi K, Ikuta T, Abe H and Shimizu T 2005 *Phys. Rev. Lett.* **95** 065502
[24] Yang J, Yang Y, Waltermire S W, Wu X, Zhang H *et al.* 2012 *Nat. Nanotechnol.* **7** 91
[25] Zhang Q, Liu C, Liu X, Liu J, Cui Z *et al.* 2018 *ACS Nano* **12** 2634
[26] Sun T, Wang J and Kang W 2013 *Nanoscale* **5** 128
[27] Su R, Yuan Z, Wang J and Zheng Z 2015 *Phys. Rev. E* **91** 012136
[28] Wang X, Kaviany M and Huang B 2017 *Nanoscale* **9** 18022
[29] Liu Y, Ma Y, Zhao Y, Sun X, Gandara F *et al.* 2016 *Science* **351** 365
[30] Tavakkoli K G A, Nicaise S M, Gadelrab K R, Alexander-Katz A, Ross C A and Berggren K K 2016 *Nat. Commun.* **7** 10518
[31] Lee J H, Koh C Y, Singer J P, Jeon S J, Maldovan M, Stein O and Thomas E L 2014 *Adv. Mater.* **26** 532
[32] Kubo R 1957 *J. Phys. Soc. Jpn.* **12** 570
[33] Plimpton S 1995 *J. Comput. Phys.* **117** 1
[34] Narayan O and Ramaswamy S 2002 *Phys. Rev. Lett.* **89** 200601
[35] Kundu A, Dhar A and Narayan O 2009 *J. Stat. Mech.: Theory Exp.* **2009** L03001
[36] Das S G, Dhar A and Narayan O 2014 *J. Stat. Phys.* **154** 204
[37] Tang N, Peng Z, Guo R, An M, Chen X, Li X, Yang N and Zang J 2017 *Polymers* **9** 688
[38] Li S, Yu X, Bao H and Yang N 2018 *J. Phys. Chem. C* **122** 13140
[39] Stuart S J, Tutein A B and Harrison J A 2000 *J. Chem.*

Phys. **112** 6472
[40] Henry A, Chen G, Plimpton S J and Thompson A 2010 *Phys. Rev. B* **82** 144308
[41] Brenner D W, Shenderova O A, Harrison J A, Stuart S J, Ni B and Sinnott S B 2002 *J. Phys.: Condens. Matter* **14** 783
[42] Liu A and Stuart S J 2008 *J. Comput. Chem.* **29** 601
[43] Henry A and Chen G 2008 *Phys. Rev. Lett.* **101** 235502
[44] Ye Z Q, Cao B Y, Yao W J, Feng T and Ruan X 2015 *Carbon* **93** 915
[45] Zhang T and Luo T 2012 *J. Appl. Phys.* **112** 094304
[46] Liao Q, Liu Z, Liu W, Deng C and Yang N 2015 *Sci. Rep.* **5** 16543
[47] Yang N, Xu X, Zhang G and Li B 2012 *AIP Adv.* **2** 041410
[48] Parrish K D, Jain A, Larkin J M, Saidi W A and McGaughey A J H 2014 *Phys. Rev. B* **90** 235201
[49] Shulumba N, Hellman O and Minnich A J 2017 *Phys. Rev. Lett.* **119** 185901
[50] Wang L and Li B 2008 *Phys. Rev. Lett.* **101** 267203
[51] Liao B, Qiu B, Zhou J, Huberman S, Esfarjani K and Chen G 2015 *Phys. Rev. Lett.* **114** 115901
[52] Oyake T, Feng L, Shiga T, Isogawa M, Nakamura Y and Shiomi J 2018 *Phys. Rev. Lett.* **120** 045901
[53] Liao B, Zhou J and Chen G 2014 *Phys. Rev. Lett.* **113** 025902
[54] Tamm A, Caro M, Caro A, Samolyuk G, Klintenberg M and Correa A A 2018 *Phys. Rev. Lett.* **120** 185501
[55] Ihle D 1977 *Phys. Status Solidi B* **80** 619
[56] Waldecker L, Bertoni R, Hubener H, Brumme T, Vasileiadis T, Zahn D, Rubio A and Ernstorfer R 2017 *Phys. Rev. Lett.* **119** 036803
[57] Ma W L, Yang C Y, Gong X, Lee K and Heeger A J 2005 *Adv. Funct. Mater.* **15** 1617
[58] Furchi M M, Pospischil A, Libisch F, Burgdorfer J and Mueller T 2014 *Nano Lett.* **14** 4785

Supplementary Information: How Does van der Waals Confinement Enhance Phonon Transport?

Xiaoxiang Yu (余晓翔)[1, 2, #], Dengke Ma (马登科)[1, 3, #], Chengcheng Deng (邓程程)[2, *], Xiao Wan (万骁)[2], Meng An (安盟)[1, 4], Han Meng (孟涵)[2], Xiaobo Li (李小波)[2], Xiaoming Huang (黄晓明)[2 *], and Nuo Yang (杨诺)[1, 2, *]

[1] State Key Laboratory of Coal Combustion, Huazhong University of Science and Technology, Wuhan 430074, P. R. China

[2] School of Energy and Power Engineering, Huazhong University of Science and Technology, Wuhan 430074, P. R. China

[3] NNU-SULI Thermal Energy Research Center (NSTER) & Center for Quantum Transport and Thermal Energy Science (CQTES), School of Physics and Technology, Nanjing Normal University, Nanjing, 210023, P. R. China

[4] College of Mechanical and Electrical Engineering, Shaanxi University of Science and Technology, Xi'an 710021, China

Simulation Structure

The Simulation structures of CPL-PE and CPL-GNR are shown as below.

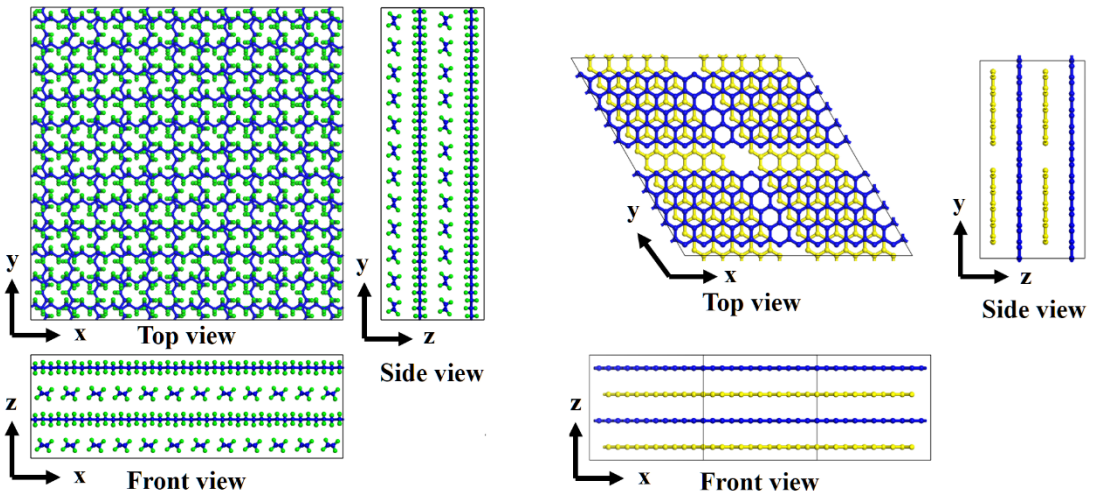

FIG. S1. Three views of CPL-PE and CPL-GNR.

Relaxation in NPT Ensemble

To get the relaxed CPL-PE structure, initial structure is minimized by standard conjugate-gradient energy-minimization method in LAMMPS. Then, the system runs in isobaric-isothermal ensemble (NPT) for 100 ps. Fig. S2 shows the stress as a function of time, indicating no stress in all three directions after NPT process. For CPL-PE simulation system, the average system size after relaxation is 5.16 nm × 3.42 nm × 5.16 nm. Its chain is 20-unit-cell long with initial length of 5.10 nm, which denotes a slight tensile strain of 1.2% that almost has no influence on the TC of PE chain [1].

As for the thermodynamic stability, we agree that simulation system should run for long enough time (far beyond MD time scale) to achieve a stable state. In this work, we performed NPT relaxation process and obtained a reasonable mass density (0.975 g/cm^3). Moreover, we conducted the MD simulation at wide temperature range (250K – 400K) and the CPL-PE structure still keeps stable at high temperature (400K).

The CPL structures are probably fabricated according to a recent experimental research on the weaving of organic threads [2]. Previous experiments also reported many analogous structures such as orthogonal self-assembly multilayer polymer meshes [3] and ordered polymer structure [4], which exemplified that such kind of structures could be thermodynamically stable.

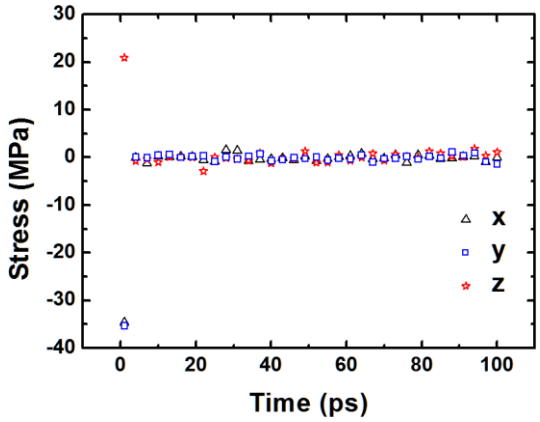

FIG. S2. Stress of CPL-PE system during NPT relaxation process.

Simulation Details

Table S1. Parameter settings in MD simulation.

Method	Equilibrium MD (Green-Kubo method)		Potential	AIREBO	
Simulation process					
Ensemble	Setting				Purpose
NPT	Time step (fs)	0.1	Runtime (ns)	0.1	Relax structure
	Temperature (K)	300	Pressure (atm)	0	
	Boundary condition	X, Y, Z: periodic, periodic, periodic			
NVT	Time step (fs)	0.1	Runtime (ns)	0.01	Relax structure
	Temperature (K)	300	Thermostat	Nose Hoover	
	Boundary condition	X, Y, Z: periodic, periodic, periodic			
NVE	Sample interval time (fs)	1	Runtime (ns)	5	Record trajectory
	Correlation time (ps)	500	Temperature (K)	300	
	Boundary condition	X, Y, Z: periodic, periodic, periodic			

In all simulations, The velocity Verlet algorithm [5] is employed to integrate equations of motion. The initial conditions for all simulations use the conjugate gradient minimized equilibrium positions and random velocities corresponding to given temperatures. The system runs in isobaric–isothermal ensemble at 0 bar for 100 picoseconds with different initial conditions (see Fig. S1). We used a 0.1 femtosecond time step and recorded the trajectories every 1 femtosecond at equilibrium state in microcanonical ensemble for 5 nanoseconds with total energy mean variance of 0.005%. The Green-Kubo formula relates the equilibrium fluctuations of heat current, in terms of autocorrelation function, to thermal conductivity via the fluctuation-dissipation theorem. Based on the lattice parameters of ideal PE crystal, the cross-sectional-area of SC-PE is set as 18 $Å^2$ [6]. We used a combination of time

and ensemble sampling to obtain a better average statistics. The results presented are averaged over 5 independent simulations with different initial conditions.

Chain Length Dependence of κ

In order to get the appropriate system length for EMD simulations, the size dependence of thermal conductivity of SC-PE, Array-PE, CPL-PE and CPL-GNR at 300 K are presented in Fig. S3. Moreover, $\kappa_{SC\text{-}PE}$, $\kappa_{Array\text{-}PE}$, $\kappa_{CPL\text{-}PE}$ and $\kappa_{CPL\text{-}GNR}$ almost converge with chain length longer than 5nm. Therefore, 5 nm length is selected to overcome the finite size effect.

There is two widely used molecular dynamics simulation methods, non-equilibrium molecular dynamics (NEMD) and equilibrium molecular dynamics (EMD). In our manuscript, EMD is preferred, instead of NEMD used in Ref. [7].

The advantage of EMD is to simulate a 1D structure (nanotube/single-chain) with an infinite length or a bulk structure [8-10], where a periodic boundary conditions is used. That is, the phonons will not be scatted at the boundaries. When the simulation cell is large enough, the calculated value of thermal conductivity converges due to a competing effect of increasing on both phonon modes and scatterings [7, 11, 12]. In our work, Fig. S3 shows that thermal conductivity of single chain converges and is almost independent of the simulation length when the simulation cell is larger than 5 nm. Liao et al. also reported [13] a similar result of PE single chain by EMD.

However, the EMD is not good in study a nanostructure with a finite length where the size effect is important. The phonons are scattered at boundaries, which confines phonon mean free paths. In such cases, it is well simulated by NEMD method [7, 14]. Ref. [15] reported that thermal conductivity of single PE chain increased with its length by NEMD method with a fixed boundary conditions.

More details about EMD and NEMD can be found in Ref. [7, 12].

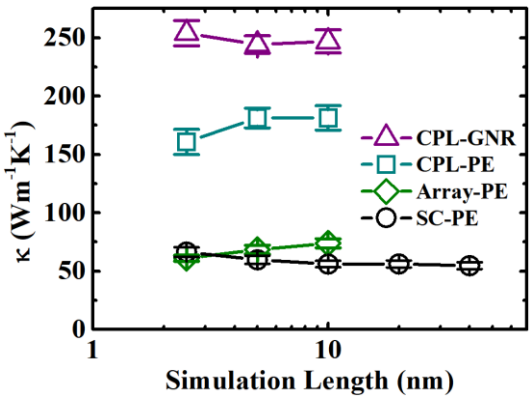

FIG. S3. Size dependence of thermal conductivity of SC-PE, Array-PE, CPL-PE and CPL-GNR.

Radial Distribution Function (RDF)

The reference atom (x_0, y_0, z_0) is the average coordinates of all atoms. We select a chain along x direction in CPL-PE. RDF is calculated according to the formula of $g(r) = N/(2n\text{-}1)$. The distance (r) is defined as $r = [(y\text{-}y_0)^2 + (z\text{-}z_0)^2]^{1/2}$. N is the count of atoms in nth annulus ($R \leq r < R + d$). $A(r)$ is the area of annulus. The width of each annulus (d) is set to 0.2 Å. The value of πd^2 is normalized as 1, thus the area of nth annulus is $A(r) = \pi(nd)^2 - \pi[(n\text{-}1)d]^2 = (2n\text{-}1)\pi d^2$.

Local vdW Potential Barrier

Firstly, we move a PE chain along z axis in CPL-PE or Array-PE translationally for a distance of 0.01 Å per step within a range of 2 Å × 2 Å in yz-plane and calculate the potential energy of the PE chain. Then we rotate the same PE chain while keeping other chains static to attain the angle dependence of potential energy change.

To evaluate the effect of thermal fluctuation, the vdW potential barriers at 300 K are calculated. The CPL-PE and Array-PE systems run for 50 picoseconds, and 50 configurations are sampled per 1 picosecond. Then, the vdW potential barriers of every configuration are calculated. Finally, the averaged vdW potential barriers of 50 configurations are obtained. As shown in Fig. S4, compared with static structures at 0 K, the vdW potential barriers with thermal fluctuation (at 300 K) are higher in CPL and array structures, which is due to the internal energy of atomic thermal motions. Similar to those in static structures (a), confined vdW potential barriers exist in CPL structures at 300 K (c), which verifies that the vdW confinement effect works well with thermal fluctuation.

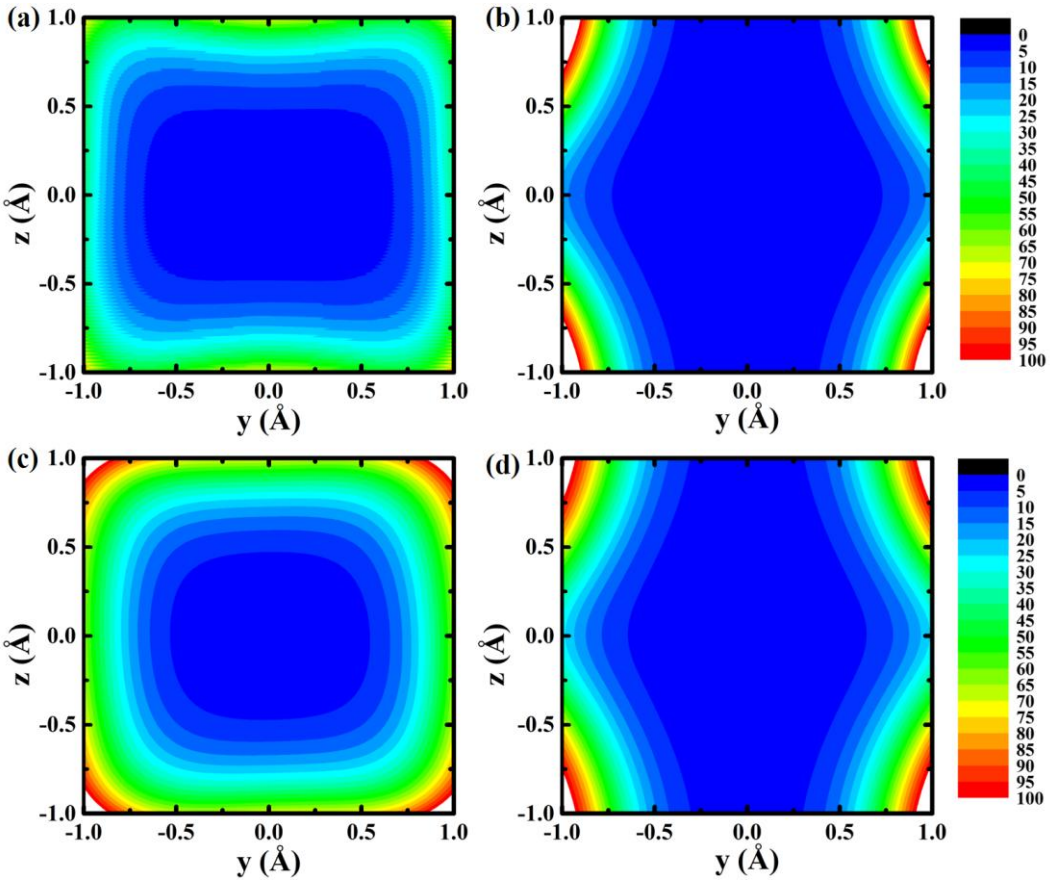

FIG. S4. The vdW potential energy barriers of PE chain in CPL-PE at (a) 0 K and (c) 300 K, and Array-PE at (b) 0 K and (d) 300 K.

Potential Barriers in GNR Systems

We calculate the potential barriers to elaborate the vdW confinement in GNR systems. As shown in Fig. S5, the mapping potential of CPL-GNR shows slight shrink from center to edge along the *z*-direction while that of Array-GNR does not. It means that, compared with array, CPL exhibits slightly stronger confinement along the *z*-direction, thus leads to slightly larger thermal conductivity.

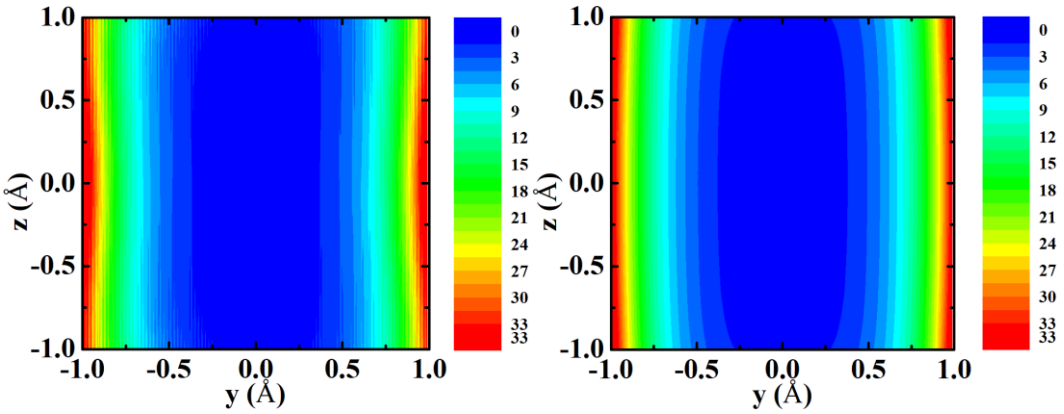

FIG. S5. The vdW potential barrier felt by GNR in array (left) and CPL (right).

# X. Y. and D. M. contributed equally to this work.

* To whom correspondence should be addressed. E-mail: dengcc@hust.edu.cn (C.D.), xmhuang@hust.edu.cn (X.H.), nuo@hust.edu.cn (N.Y.).

[1] T. Zhang and T. Luo, *Morphology-Influenced Thermal Conductivity of Polyethylene Single Chains and Crystalline Fibers*, J. Appl. Phys. **112** 094304 (2012).

[2] Y. Liu, Y. Ma, Y. Zhao, X. Sun, F. Gandara, et al., *Weaving of organic threads into a crystalline covalent organic framework*, Science **351** 365 (2016).

[3] A. Tavakkoli K. G, S. M. Nicaise, K. R. Gadelrab, A. Alexander-Katz, C. A. Ross, and K. K. Berggren, *Multilayer block copolymer meshes by orthogonal self-assembly*, Nat. Commun. **7** 10518 (2016).

[4] J. H. Lee, C. Y. Koh, J. P. Singer, S. J. Jeon, M. Maldovan, O. Stein, and E. L. Thomas, *25th anniversary article: ordered polymer structures for the engineering of photons and phonons*, Adv. Mat. **26** 532 (2014).

[5] W. C. Swope, H. C. Andersen, P. H. Berens, and K. R. Wilson, *A computer simulation method for the calculation of equilibrium constants for the formation of physical clusters of molecules: Application to small water clusters*, J. Chem. Phys. **76** 637 (1982).

[6] A. Henry and G. Chen, *High thermal conductivity of single polyethylene chains using molecular dynamics simulations*, Phys. Rev. Lett. **101** 235502 (2008).

[7] P. K. Schelling, S. R. Phillpot, and P. Keblinski, *Comparison of Atomic-Level Simulation Methods for Computing Thermal Conductivity*, Phys. Rev. B **65** 144306 (2002).

[8] A. Henry, G. Chen, S. J. Plimpton, and A. Thompson, *1D-to-3D transition of phonon heat conduction in polyethylene using molecular dynamics simulations*, Phys. Rev. B **82** 144308 (2010).

[9] L. Yang, N. Yang, and B. Li, *Extreme low thermal conductivity in nanoscale 3D Si phononic crystal with spherical pores*, Nano Lett. **14** 1734 (2014).

[10] D. Ma, H. Ding, H. Meng, L. Feng, Y. Wu, J. Shiomi, and N. Yang, *Nano-cross-junction effect on phonon transport in silicon nanowire cages*, Phys. Rev. B **94** 165434 (2016).

[11] L. Yang, N. Yang, and B. Li, *Reduction of thermal conductivity by nanoscale 3D phononic crystal*, Sci. Rep. **3** 1143 (2013).

[12] J. Che, T. Çağın, W. Deng, and W. A. Goddard, *Thermal conductivity of diamond and related materials from molecular dynamics simulations*, J. Chem. Phys. **113** 6888 (2000).

[13] Q. Liao, Z. Liu, J. Yang, and W. Liu, *Study of the dependence of the thermal conductivity of a single polyethylene chain on length, temperature, and mechanical strain using molecular dynamics simulations*, Inter. J. Ener. Clean Env. **15** 1 (2014).

[14] H. Dong, Z. Fan, L. Shi, A. Harju, and T. Ala-Nissila, *Equivalence of the equilibrium and the nonequilibrium molecular dynamics methods for thermal conductivity calculations: From bulk to nanowire silicon*, Phys. Rev. B **97** 094305 (2018).

[15] J. Liu and R. Yang, *Length-Dependent Thermal Conductivity of Single Extended Polymer Chains*, Phys. Rev. B **86** 104307 (2012).